J Antimicrob Chemother
doi:10.1093/jac/dkab072

Journal of Antimicrobial Chemotherapy

In vitro antiviral activity of the anti-HCV drugs daclatasvir and sofosbuvir against SARS-CoV-2, the aetiological agent of COVID-19

Carolina Q. Sacramento[1,2]†, Natalia Fintelman-Rodrigues[1,2]†, Jairo R. Temerozo[3,4], Aline de Paula Dias Da Silva[1,2], Suelen da Silva Gomes Dias[1], Carine dos Santos da Silva[1,2], André C. Ferreira[1,2,5], Mayara Mattos[1,2], Camila R. R. Pão[1], Caroline S. de Freitas[1,2], Vinicius Cardoso Soares[1], Lucas Villas Bôas Hoelz[6], Tácio Vinício Amorim Fernandes[6,7], Frederico Silva Castelo Branco[6], Mônica Macedo Bastos[6], Núbia Boechat[6], Felipe B. Saraiva[8], Marcelo Alves Ferreira[2,8], Steffen Jockusch[9,10], Xuanting Wang[9,11], Chuanjuan Tao[9,11], Minchen Chien[9,11], Wei Xie[12], Dinshaw Patel[12], Aitor Garzia[13], Thomas Tuschl[13], James J. Russo[9,11], Rajith K. R. Rajoli[14], Carolina S. G. Pedrosa[15], Gabriela Vitória[15], Letícia R. Q. Souza[15], Livia Goto-Silva[15], Marilia Zaluar Guimarães[15,16], Stevens K. Rehen[15,16], Andrew Owen[14], Fernando A. Bozza[15,17], Dumith Chequer Bou-Habib[3,4], Jingyue Ju[9,11,18], Patrícia T. Bozza[1] and Thiago Moreno L. Souza[1,2]*

[1]Laboratório de Imunofarmacologia, Instituto Oswaldo Cruz (IOC), Fundação Oswaldo Cruz (Fiocruz), Rio de Janeiro, RJ, Brazil; [2]National Institute for Science and Technology on Innovation in Diseases of Neglected Populations (INCT/IDPN), Center for Technological Development in Health (CDTS), Fiocruz, Rio de Janeiro, RJ, Brazil; [3]Laboratório de Pesquisas sobre o Timo, IOC, Fiocruz, Rio de Janeiro, RJ, Brazil; [4]National Institute for Science and Technology on Neuroimmunomodulation (INCT/NIM), IOC, Fiocruz, Rio de Janeiro, RJ, Brazil; [5]Universidade Iguaçu, Nova Iguaçu, RJ, Brazil; [6]Instituto de Tecnologia de Fármacos (Farmanguinhos), Fiocruz, Rio de Janeiro, RJ, Brazil; [7]Laboratório de Macromoléculas, Diretoria de Metrologia Aplicada às Ciências da Vida, Instituto Nacional de Metrologia, Qualidade e Tecnologia—INMETRO, Duque de Caxias, RJ 25250-020, Brazil; [8]Instituto de Tecnologia em Imunobiológicos (Bio-Manguinhos), Fiocruz, Rio de Janeiro, RJ, Brazil; [9]Center for Genome Technology and Biomolecular Engineering, Columbia University, New York, NY 10027, USA; [10]Department of Chemistry, Columbia University, New York, NY 10027, USA; [11]Department of Chemical Engineering, Columbia University, New York, NY 10027, USA; [12]Laboratory of Structural Biology, Memorial Sloan-Kettering Cancer Center, New York, NY 10065, USA; [13]Laboratory of RNA Molecular Biology, Rockefeller University, New York, NY 10065, USA; [14]Department of Molecular and Clinical Pharmacology, University of Liverpool, Liverpool L7 3NY, UK; [15]Instituto D'Or de Pesquisa e Ensino, Rio de Janeiro, RJ, Brazil; [16]Instituto de Ciências Biomédicas, Universidade Federal do Rio de Janeiro, Rio de Janeiro, RJ, Brazil; [17]Instituto Nacional de Infectologia Evandro Chagas, Fiocruz, Rio de Janeiro, RJ, Brazil; [18]Department of Molecular Pharmacology and Therapeutics, Columbia University, New York, NY, 10032, USA

*Corresponding author. E-mail: tmoreno@cdts.fiocruz.br
†These authors contributed equally to this work.

Received 10 October 2020; accepted 10 February 2021

Background: Current approaches of drug repurposing against COVID-19 have not proven overwhelmingly successful and the SARS-CoV-2 pandemic continues to cause major global mortality. SARS-CoV-2 nsp12, its RNA polymerase, shares homology in the nucleotide uptake channel with the HCV orthologue enzyme NS5B. Besides, HCV enzyme NS5A has pleiotropic activities, such as RNA binding, that are shared with various SARS-CoV-2 proteins. Thus, anti-HCV NS5B and NS5A inhibitors, like sofosbuvir and daclatasvir, respectively, could be endowed with anti-SARS-CoV-2 activity.

Methods: SARS-CoV-2-infected Vero cells, HuH-7 cells, Calu-3 cells, neural stem cells and monocytes were used to investigate the effects of daclatasvir and sofosbuvir. *In silico* and cell-free based assays were performed with SARS-CoV-2 RNA and nsp12 to better comprehend the mechanism of inhibition of the investigated compounds. A physiologically based pharmacokinetic model was generated to estimate daclatasvir's dose and schedule to maximize the probability of success for COVID-19.

Results: Daclatasvir inhibited SARS-CoV-2 replication in Vero, HuH-7 and Calu-3 cells, with potencies of 0.8, 0.6 and 1.1 μM, respectively. Although less potent than daclatasvir, sofosbuvir alone and combined with daclatasvir inhibited replication in Calu-3 cells. Sofosbuvir and daclatasvir prevented virus-induced neuronal apoptosis and release of cytokine storm-related inflammatory mediators, respectively. Sofosbuvir inhibited RNA synthesis by chain termination and daclatasvir targeted the folding of secondary RNA structures in the SARS-CoV-2 genome.

Concentrations required for partial daclatasvir *in vitro* activity are achieved in plasma at C_{max} after administration of the approved dose to humans.

Conclusions: Daclatasvir, alone or in combination with sofosbuvir, at higher doses than used against HCV, may be further fostered as an anti-COVID-19 therapy.

Introduction

The beginning of the 21st century has been marked by the emergence of severe acute respiratory syndrome coronavirus (SARS-CoV) in 2002, middle-east respiratory syndrome (MERS-CoV) in 2014[1] and SARS-CoV-2 currently. The SARS-CoV-2 outbreak provoked over 100 000 confirmed deaths/month associated with 2019 coronavirus disease (COVID-19).[2] To combat COVID-19, the WHO launched the global Solidarity trial, with repurposed drugs, which was unsuccessful.[3,4] Although independent clinical trials with remdesivir suggest clinical benefit,[5–7] its high price and IV administration make this drug impractical.

To expand the analysis to other products with the potential to be repurposed against COVID-19, drugs approved in the last 5 years against HCV with an acceptable safety profile are worth testing.[8] Due to their recent incorporation among therapeutic agents, drugs like daclatasvir and sofosbuvir have not been systematically tested against SARS-CoV or MERS-CoV.

Daclatasvir inhibits HCV replication by binding to the N-terminus of non-structural protein 5A (NS5A), affecting both viral RNA replication and virion assembly.[8] NS5A is a multifunctional protein involved in the HCV replicative cycle and related cellular steps, as well as antagonism of IFN pathways.[8] SARS-CoV-2, which has a genome 3 times larger than HCV, expresses the non-structural proteins (nsp) 1 to 16, with similar functions compared with HCV's NS5A.[9] Sofosbuvir inhibits the HCV RNA polymerase (NS5B)[10] and the replication of Zika, yellow fever and chikungunya viruses.[11–14] Sofosbuvir is a pro-drug that enter cells due to its hydrophobic protections in its phosphate and must be converted into the active triphosphorylated nucleotide (sofosbuvir-TP) by cellular enzymes cathepsin A (CatA), carboxylesterase 1 (CES1) and histidine triad nucleotide-binding protein 1 (Hint1), classically expressed in the liver,[15] but also present in other tissue, such as the respiratory tract.[16–18] Moreover, similarities between the SARS-CoV-2 and HCV RNA polymerase provide a rationale for studying sofosbuvir against COVID-19.[19] Indeed, enzymatic assays demonstrated sofosbuvir acts as a competitive inhibitor of SARS-CoV-2 RNA polymerase.[20,21]

Taken collectively, we describe (for the first time, to the best of our knowledge) the susceptibility of SARS-CoV-2 to daclatasvir and sofosbuvir in relevant cell types, such as Calu-3 type II pneumocytes. Our results reveal cooperative action of these drugs against SARS-CoV-2 replication, preventing virus-induced neuronal apoptosis and release of cytokine storm-related inflammatory mediators. Whereas sofosbuvir inhibits SARS-CoV-2 RNA synthesis as a chain terminator, daclatasvir favours the unfolding of viral secondary RNA structures in the SARS-CoV-2 genome and inhibits the virus's polymerase reaction. Concentrations required for partial daclatasvir *in vitro* activity can be achieved in plasma at C_{max} after administration of the approved dose to humans.

Materials and methods

Reagents

A list of reagents is described in Table S1 (available as Supplementary data at *JAC* Online).

Methods

The detailed methods are described in the Supplementary Materials and methods available at *JAC* Online. The most significant aspects are described in brief in this section.

In vitro assays

African green monkey kidney cells (Vero cells, subtype E6), human lung epithelial cells (A549 and Calu-3 cells), human hepatoma lineage cells (HuH-7 cells), human primary monocytes and 2D and 3D culture systems of human neural stem cells (NSCs) derived from induced pluripotent stem (iPS) cells were used to evaluate antiviral susceptibility to SARS-CoV-2 (isolated from a nasopharyngeal swab from a confirmed case in Rio de Janeiro, Brazil—GenBank MT710714).

Cells were infected at different MOIs for 1 h at 37°C, treated and cultured from 1 to 5 days after infection. From culture supernatants, infectious virus titres and RNA levels were determined by plaque assay or qRT–PCR, respectively.[22] Supernatant was assayed to monitor TNF and IL-6 levels by ELISA. Cell monolayers were lysed and SARS-CoV-2 genomic (ORF1b)/subgenomic (ORFE) RNA levels were quantified by qRT–PCR.[23] Alternatively, monolayers were assayed for cell death by XTT or TUNEL methods.

Generation of SARS-CoV-2 mutants

SARS-CoV-2 mutants, grown in the presence of daclatasvir, were generated from the sequential passages of SARS-CoV-2 in Vero cells in the presence of increasing concentrations of the drug. Virus RNA recovered from the supernatants of each passage underwent unbiased sequencing using an MGI-2000 and a metatranscriptomics approach.

Assay for inhibition of SARS-CoV-2 RNA-dependent RNA polymerase (RdRp)

The pre-assembled SARS-CoV-2 RdRp complex (nsp12/nsp7/nsp8)[24,25] was incubated with appropriate concentrations of aqueous daclatasvir dihydrochloride for 15 min at room temperature in reaction buffer. Then the annealed RNA template-loop-primer in reaction buffer was added to the RdRp-daclatasvir mixture and incubated for an additional 10 min at room temperature. Finally, UTP or sofosbuvir-TP was added and incubation was carried out for 1 h at 30°C. The final concentrations of the reagents in the 20 μL extension reactions were 1 μM RdRp complex (nsp12/nsp7/nsp8), 500 nM RNA template-loop-primer, 0, 1, 4, 16 or 64 μM daclatasvir and 3 μM UTP or 15 μM sofosbuvir-TP. Following desalting, the samples were subjected to MALDI-TOF MS analysis.

Melting curve assay

Melting profiles were obtained by incubating SARS-CoV-2 RNA with daclatasvir and SYBR Green in a StepOne™ Real-Time PCR System programmed with a default melting curve.

Molecular docking

The structures of the active metabolite of sofosbuvir (sofosbuvir-TP) and daclatasvir were constructed, optimized and docked into the crystal structure of the SARS-Cov-2 nsp12 from Protein Data Bank (7BV2)[19] or into viral RNA using the Molegro Virtual Docker 6.0 software.[26] Also, daclatasvir was docked to the crystal structure of SARS-CoV-2 RNA (6XRZ)[27] using the same software.

Physiologically based pharmacokinetic (PBPK) model

A daclatasvir whole-body PBPK model was constructed in Python 3.5 The PBPK model was constructed based on a few assumptions: (i) uniform and instant distribution across a given tissue; (ii) no reabsorption from the colon; and (iii) the model was blood-flow limited. The model simulations, validations and predictions are detailed in the Supplementary Materials and methods available at *JAC* Online. The simulated data in humans are computer generated, so no ethical approval was required for this study.

Results

Daclatasvir is more potent than sofosbuvir in inhibiting the production of infectious SARS-CoV-2

SARS-CoV-2 may infect cell lineages from different organs, but permissive production of infectious virus particles may vary. Vero E6, HuH-7 and Calu-3 cells produced infectious SARS-CoV-2 titres and quantifiable RNA levels (Figure S1), showing they sustain permissive replication. On the other hand, A549 cells, NSCs and monocytes displayed limited ability to generate virus progeny, as measured by pfu (Figure S1A).

Next, the phenotypic experiments were performed at an MOI of 0.01 for Vero cells 24 h after infection and 0.1 for HuH-7 and Calu-3 cells 48 h after infection. Daclatasvir consistently inhibited the production of SARS-CoV-2 infectious virus titres in a dose-dependent manner in all tested cell types (Figure 1), being similarly potent in Vero, HuH-7 and Calu-3 cells, with EC_{50} values ranging from 0.6 to 1.1 μM (Table 1). Daclatasvir showed limited antiviral activity based on viral RNA copies/mL in the culture supernatant fraction (Figure S2).

SARS-CoV-2 susceptibility to sofosbuvir in HuH-7 and Calu-3 cells was lower compared with daclatasvir (Figure 1b and d and Table 1). Because Vero cells poorly activate sofosbuvir to its active triphosphate, sofosbuvir did not affect SARS-CoV-2 replication in these cells. Similar to what was observed for daclatasvir, quantification of sofosbuvir's antiviral activity by pfu was more sensitive than by viral RNA quantification in the supernatant fraction (Figure S2). Daclatasvir was at least 7 times more potent than sofosbuvir in HuH-7 and Calu-3 cells (Table 1).

Sofosbuvir's nucleoside metabolite (GS-331007; Figure S3) was also inactive in Vero cells and less active than sofosbuvir in HuH-7 cells (Figure 1 and Table 1).

Given that SARS-CoV-2 replication in Calu-3 cells appeared to be more sensitive to antiviral activity, this cell line was used to assess the combination of sofosbuvir and daclatasvir. Sofosbuvir/daclatasvir was used at ratios of 1:0.15 and 1:1, to mimic the dosage proportions for HCV-positive patients (400 mg of sofosbuvir plus 60 mg of daclatasvir) and their plasma exposure, respectively.[28] In this assessment of the interaction, the potency of sofosbuvir increased from 10- to 35-fold in the presence of suboptimal daclatasvir concentrations (Figure 1c and e and Table 1), suggesting at least some synergistic effect (Table 1).

Daclatasvir was more potent than the positive controls ribavirin, chloroquine and lopinavir/ritonavir, proportion of 4:1, which is equivalent to the dosage approved for HIV patients[29] and suggested for SARS-CoV-2 in the WHO's Solidarity trial[4] (100 mg of lopinavir plus 25 mg of ritonavir) (Figure 1 and Table 1), whereas sofosbuvir potency was similar to that of ribavirin in HuH-7 and Calu-3 cells (Figure 1 and Table 1). However, the selectivity index ($SI = CC_{50}/EC_{50}$) for sofosbuvir was 4.6-fold superior to ribavirin, because of sofosbuvir's lower cytotoxicity (Table 1). None of the studied drugs was more potent than remdesivir (Figure 1 and Table 1).

These data demonstrate that SARS-CoV-2 is susceptible to daclatasvir and sofosbuvir *in vitro*, with daclatasvir having a higher potency than sofosbuvir, and the highest potency achieved by the combination of daclatasvir and sofosbuvir in Calu-3 cells.

Protective effect of sofosbuvir and daclatasvir in non-permissive cells

Although productive replication of SARS-CoV-2 in neurons and monocytes was not observed (Figure S1), these cells were associated with neuro-COVID-19[30] and cytokine storm,[31] respectively. Sofosbuvir reduced SARS-CoV-2 RNA levels by 20%–40% in 2D NSCs, at a concentration of 1 μM (Figure 2a). Conversely, no impact of daclatasvir on SARS-CoV-2 RNA levels was observed in NSCs (Figure 2a). Using the more physiological NSC-based 3D neurosphere system, SARS-CoV-2-induced apoptosis (TUNEL-positive nuclei over total nuclei) was prevented by sofosbuvir (Figure 2b), whereas benefits of daclatasvir in this system were limited.

In SARS-CoV-2-infected human primary monocytes, 1 μM daclatasvir reduced viral RNA levels/cell (Figure 3a), whereas sofosbuvir was inactive. Daclatasvir also reduced the SARS-CoV-2-induced enhancement of TNF-α and IL-6 (Figure 3b and c). These data provide further evidence for a putative benefit in COVID-19 with the investigated HCV antivirals, if target concentrations can be achieved in patients.

Daclatasvir and sofosbuvir inhibit early events during SARS-CoV-2 replication

The observation that suboptimal concentrations of daclatasvir augmented the antiviral activity of sofosbuvir (Figure 1c and f) may indicate that they target different processes during viral replication. Sofosbuvir competitively inhibits SARS-CoV-2 RNA polymerase.[20] In HCV, daclatasvir blocks the multi-functional protein NS5A, also suggesting these agents target different mechanisms within the SARS-CoV-2 life cycle. To gain insights on the temporality of daclatasvir's activity against SARS-CoV-2, Vero cells were infected at an MOI of 0.01 and treated at different timepoints, with daclatasvir at 2-fold its EC_{50}. This time-of-addition assay demonstrated that daclatasvir treatment could be efficiently postponed up to 4 h, similarly to ribavirin, a pan-RNA polymerase inhibitor

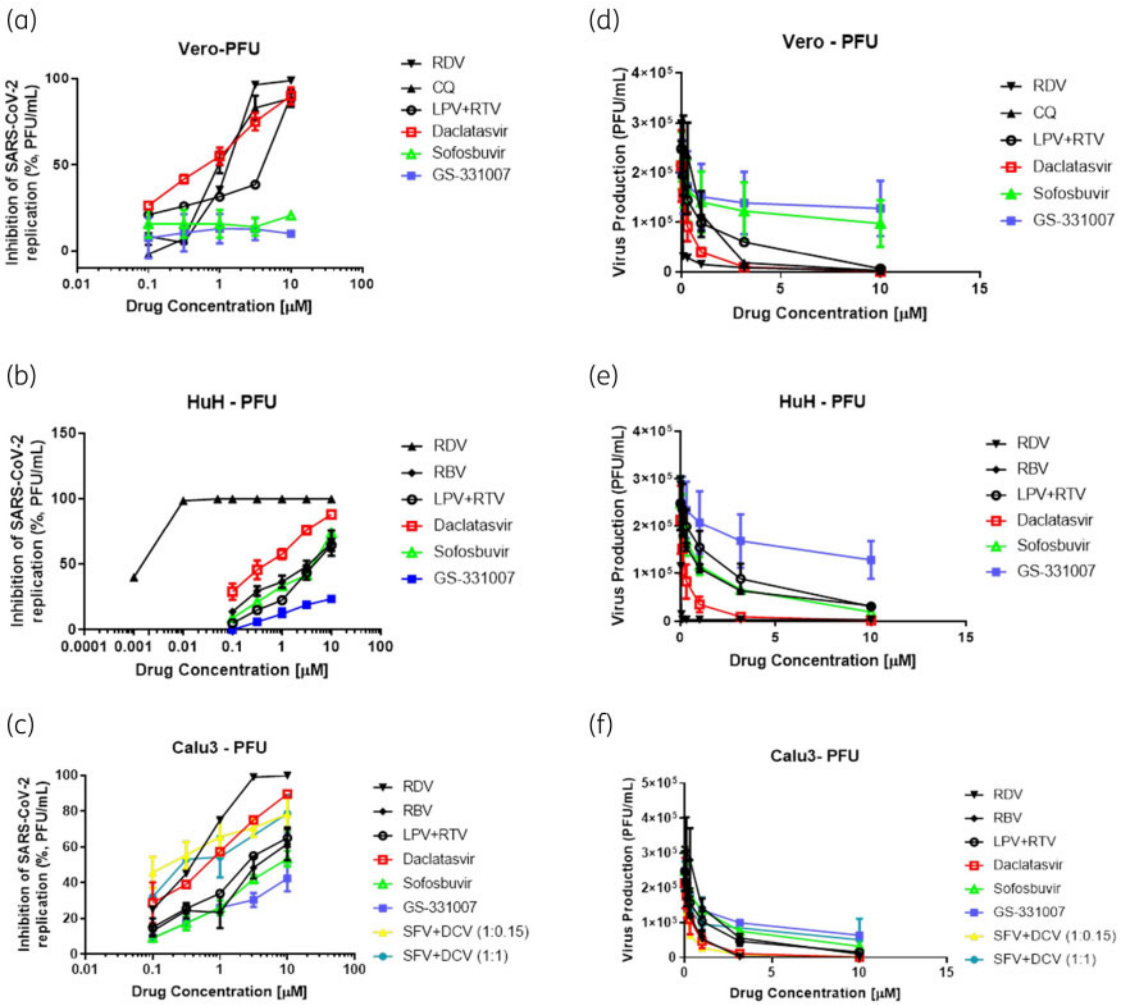

Figure 1. Antiviral activity of daclatasvir and sofosbuvir against SARS-CoV-2. Vero (a and d), HuH-7 (b and e) or Calu-3 (c and f) cells, at a density of 5×10^5 cells/well in 48-well plates, were infected with SARS-CoV-2, for 1 h at 37°C. An inoculum was removed and cells were washed and incubated with fresh DMEM containing 2% FBS and the indicated concentration of daclatasvir, sofosbuvir, sofosbuvir's nucleoside (GS-331007), chloroquine (CQ), lopinavir/ritonavir (LPV+RTV), ribavirin (RBV), remdesevir (RDV) or sofosbuvir/daclatasvir (SFV+DCV) (proportion of 1:0.15 or 1:1). Vero cells (a and d) were infected at an MOI of 0.01 and supernatants were assessed after 24 h. HuH-7 (b and e) and Calu-3 (c and f) cells were infected at an MOI of 0.1 and supernatants were assessed after 48 h. Viral replication in the culture supernatant was measured by pfu/mL. Results are displayed as percentage of inhibition (a–c) or virus titres (d–f). The data represent means±SEM of three independent experiments. This figure appears in colour in the online version of *JAC* and in black and white in the print version of *JAC*.

(Figure 4a). These results suggest that inhibition of viral RNA synthesis is the limiting event targeted by daclatasvir.

As judged by the intracellular levels of SARS-CoV-2 genomic and subgenomic RNA measured in Calu-3 cells, sofosbuvir and daclatasvir inhibit early events in the viral life cycle (Figure 4b). A 2-fold higher inhibition of viral RNA synthesis was observed for daclatasvir compared with sofosbuvir (Figure 4b), when both were tested at 10 μM. Sofosbuvir/daclatasvir cooperatively inhibited SARS-CoV-2 RNA synthesis, even at 1 μM, also supporting different targets for each agent during replicase activity.

Molecular docking methods were applied to predict the complexes with lowest energy interactions between the SARS-CoV-2 RNA polymerase and sofosbuvir triphosphate (sofosbuvir-TP) and daclatasvir. Sofosbuvir-TP and daclatasvir presented rerank scores of −74.09 and −84.64 a.u., respectively. Hydrogen bond (H-bond), electrostatic and steric interactions were mapped using a ligand-map algorithm.[26] Sofosbuvir-TP was predicted to interact via H-bond with Arg553, Cys622, Asp623 and Asn691 residues and with U20 RNA nucleotide (H-bond interaction energy = −3.50 a.u.), also presenting electrostatic interactions with Lys551, Arg553 and with the two Mg^{2+} ions (electrostatic interaction energy = −13.14 a.u.), as described by Gao *et al.*,[19] and steric interactions with Arg553, Cys622, Asp623 and Asn691 residues (steric interaction energy = −74.09 a.u.) (Figure 5a–c). Furthermore, these predictions indicated that daclatasvir may interact with viral RNA in the cleft of the SARS-CoV-2 RNA polymerase (Figure 5d and e), with anchoring through H-bonds with Tyr546 and Thr687 residues, and with U9 RNA nucleotide (H-bond interaction energy = 3.68 a.u.), and also showing steric interactions with Tyr546 and Thr687 residues (steric interaction energy = −84.64 a.u.) (Figure 5d and e).

Table 1. Pharmacological parameters of SARS-CoV-2-infected cells in the presence of daclatasvir and sofosbuvir

	Vero			HuH-7			Calu-3		
Drugs	EC_{50} (μM)	CC_{50} (μM)	SI	EC_{50} (μM)	CC_{50} (μM)	SI	EC_{50} (μM)	CC_{50} (μM)	SI
DCV	0.8 ± 0.3	31 ± 8	39	0.6 ± 0.2	28 ± 5	47	1.1 ± 0.3	38 ± 5	34
SFV	>10	360 ± 43	ND	5.1 ± 0.8	381 ± 34	74	7.3 ± 0.5	512 ± 34	70
SFV/DCV (1:0.15)	ND	ND	ND	ND	ND	ND	0.7 ± 0.2[a]	389 ± 12	555
SFV/DCV (1:1)	ND	ND	ND	ND	ND	ND	0.5 ± 0.1[a]	389 ± 10	778
GS-331007	>10	512 ± 24	ND	>10	421 ± 18	ND	9.3 ± 0.2	630 ± 34	68
RBV	ND	ND	ND	6.5 ± 1.3	142 ± 12	13	7.1 ± 0.5	160	16
CQ	1.3 ± 0.4	268 ± 23	206	ND	ND	ND	ND	ND	ND
LPV/RTV	5.3 ± 0.5	291 ± 32	54	2.9 ± 0.2	328 ± 16	113	8.2 ± 0.3	256 ± 17	31

DCV, daclatasvir; SFV, sofosbuvir; GS-331007, sofosbuvir's nucleoside; RBV, ribavirin; CQ, chloroquine; LPV/RTV, lopinavir/ritonavir; ND, not determined.
[a]$P < 0.05$ comparing sofosbuvir/daclatasvir combination with sofosbuvir alone.

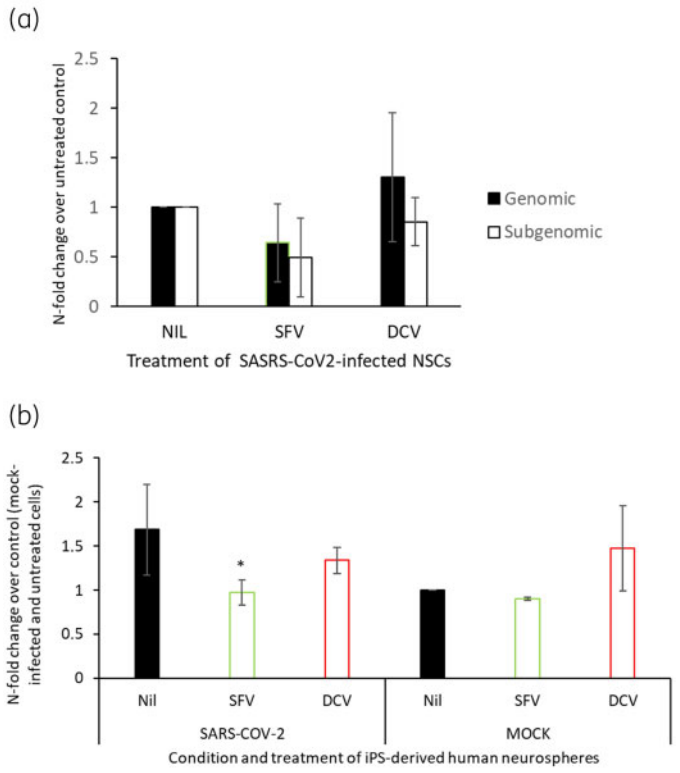

Figure 2. Sofosbuvir inhibits SARS-CoV-2 replication in human iPS cell-derived NSCs. (a) NSCs were infected at an MOI of 0.1 and treated with 1 μM sofosbuvir (SFV) or daclatasvir (DCV). After 5 days, the culture supernatants were collected and the virus was quantified by RNA levels using RT–PCR. (b) NSCs in spheroid format were labelled for TUNEL and DAPI 5 days post-infection. The data represent means±SEM of three independent experiments. An asterisk indicates $P < 0.05$ for the comparison between the SARS-CoV-2-infected cells that were untreated (Nil) versus treated with sofosbuvir. This figure appears in colour in the online version of *JAC* and in black and white in the print version of *JAC*.

Molecular docking methods were also applied to predict the complex with the lowest energy between the SARS-CoV-2 RNA and daclatasvir. Thus, daclatasvir seems to form a stable complex with viral RNA (rerank score = −96.92 a.u.) (Figure 5f) through H-bonds with G19, U20, G21, A39, C40, C43 and C46 nucleotides (H-bond interaction energy = −16.19 a.u.) (Figure 5f).

Sofosbuvir and daclatasvir inhibit the RNA synthesis catalysed by the SARS-CoV-2 RdRp complex

Sofosbuvir has been shown to act as a chain terminator during SARS-CoV-2 RNA synthesis, due to its incorporation into the newly synthesized genome.[20,24,32] After demonstrating the inhibition of viral replication by sofosbuvir and daclatasvir in various cell lines, we set out to determine at the molecular level whether daclatasvir is able to inhibit the RdRp complex (nsp12, nsp7, nsp8)-catalysed reaction, in line with molecular docking. We carried out a single base polymerase extension reaction in which UTP is incorporated into an RNA template-loop-primer by the SARS-CoV-2 RdRp complex. We compared the efficiency of extension by UTP (Figure 6) and sofosbuvir-TP (Figure S4) in the absence and presence of various concentrations of daclatasvir.

A mixture of RNA template-loop-primer (Figure 6a), SARS-CoV-2 pre-assembled RdRp complex (nsp12/nsp7/nsp8) and UTP was incubated in buffer solution at 30°C for 1 h in the absence (Figure 6b) or presence of various concentrations of daclatasvir (Figure 6c–f). The RNA template-loop-primer and the products of the polymerase extension reaction were analysed by MALDI-TOF MS (Figure 6). Addition of daclatasvir reduced the amount of the U extended RNA product peak (8157 Da expected) in a concentration-dependent manner (Figure 6g), with concomitant decreases in the unextended primer peak (7851 Da expected). Similar results were obtained for extension with sofosbuvir-TP as indicated in Figure S4. Based on these results, it is estimated that ∼2 μM daclatasvir led to 50% inhibition of the polymerase reaction catalysed by a 1 μM RdRp complex. These results suggest that daclatasvir can inhibit the reaction catalysed by the SARS-CoV-2 RdRp complex. Although both sofosbuvir and daclatasvir inhibit the reaction catalysed by the SARS-CoV-2 RdRp complex, they accomplish this by different mechanisms. Sofosbuvir is incorporated into the RNA chain where it terminates further RNA synthesis, a process which can be rescued by the SARS-CoV-2 exonuclease.[33] Daclatasvir may inhibit appropriate RdRp complex formation (nsp7/nsp8/nsp12) or the RdRp complex in combination with a

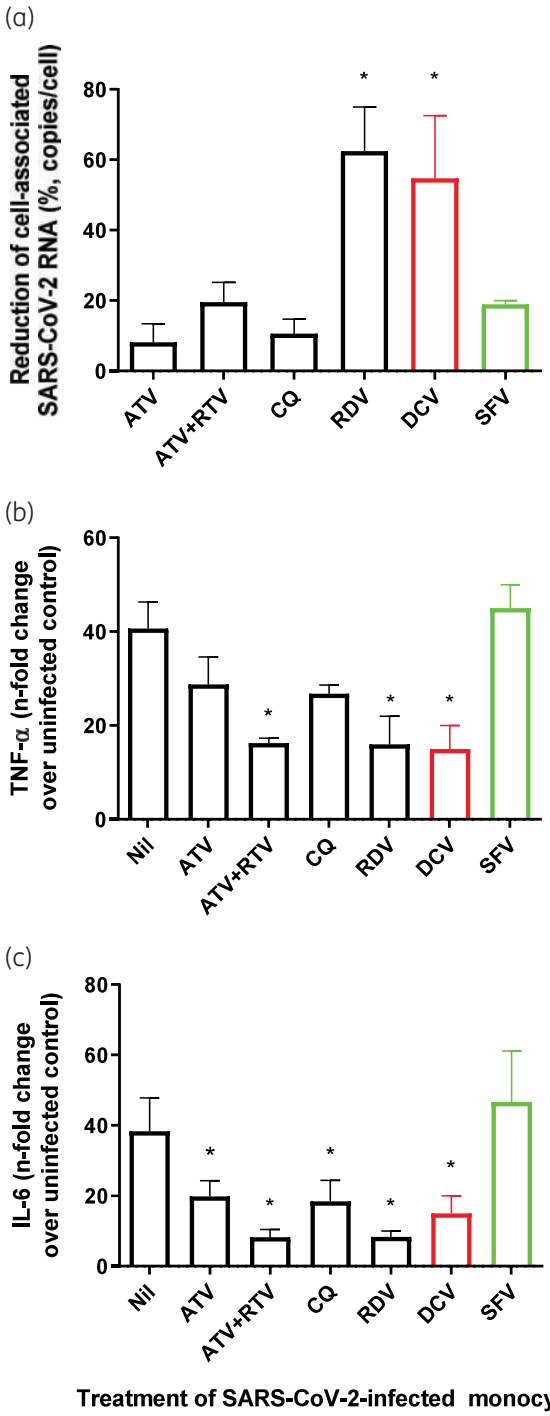

Figure 3. Daclatasvir impairs SARS-CoV-2 replication and cytokine storm in human primary monocytes. Human primary monocytes were infected at an MOI of 0.01 and treated with 1 μM daclatasvir (DCV) sofosbuvir (SFV), chloroquine (CQ), remdesevir (RDV) atazanavir (ATV) or atazanavir/ritonavir (ATV+RTV). After 24 h, cell-associated virus RNA loads (a) as well as TNF-α (b) and IL-6 (c) levels in the culture supernatant were measured. The data represent means±SEM of experiments with cells from at least three healthy donors. Differences with $P < 0.05$ are indicated with an asterisk, when compared with untreated cells (Nil) for each specific treatment. This figure appears in colour in the online version of *JAC* and in black and white in the print version of *JAC*.

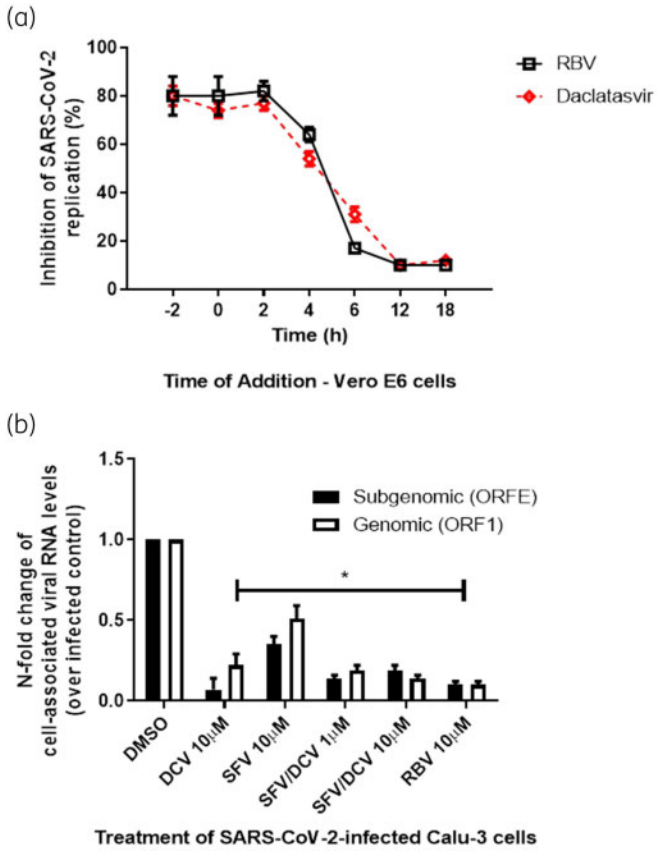

Figure 4. Daclatasvir and sofosbuvir reduced SARS-CoV-2-associated RNA synthesis. (a) To initially understand the temporal pattern of inhibition promoted by daclatasvir, we performed time-of-addition assays. Vero cells were infected with an MOI of 0.01 of SARS-CoV-2 and treated with daclatasvir or ribavirin (RBV) at 2 times their EC_{50} values at different times after infection, as indicated; 24 h post-infection, culture supernatant was harvested and SARS-CoV-2 replication was measured by plaque assay. (b) Next, Calu-3 cells (5×10^5 cells/well in 48-well plates) were infected with SARS-CoV-2 at an MOI of 0.1, for 1 h at 37°C. An inoculum was removed and cells were washed and incubated with fresh DMEM containing 2% FBS and the indicated concentration of daclatasvir (DCV), sofosbuvir (SFV), sofosbuvir/daclatasvir (SFV/DCV) (proportion of 1:0.15) or ribavirin (RBV). After 48 h, cell monolayers were lysed, total RNA extracted and quantitative RT–PCR performed for detection of ORF1 and ORFE mRNA. The data represent means±SEM of three independent experiments. *$P < 0.05$ for comparisons with vehicle (DMSO). #$P < 0.05$ for differences in genomic and sub-genomic RNA. This figure appears in colour in the online version of *JAC* and in black and white in the print version of *JAC*.

primed RNA template preventing RNA synthesis. A third possibility is that daclatasvir can destabilize the essential RNA secondary structures required for genome replication, as elaborated below. These possible inhibitory effects of daclatasvir can potentially be more lethal to SARS-CoV-2, as there are currently no known mechanisms to overcome these possible inhibitory activities.

Daclatasvir may disrupt the secondary structure of SARS-CoV-2 RNA

The different effectiveness of daclatasvir in inhibiting SARS-CoV-2 replication by pfu and RNA levels in culture supernatant, the

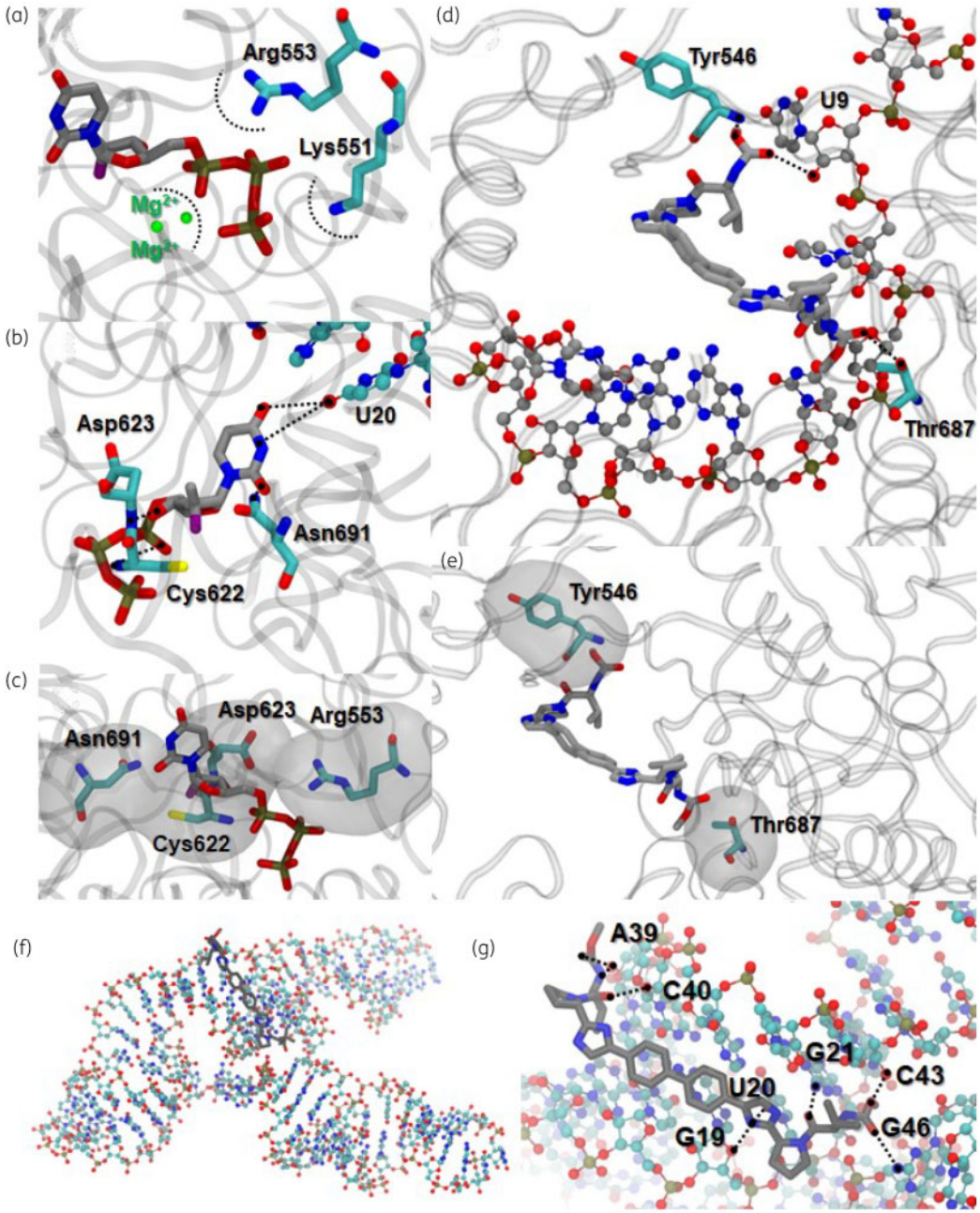

Figure 5. Representation of the predicted intermolecular interactions in the SARS-Cov-2 RNA polymerase (nsp12) complexed to the active metabolite of sofosbuvir (SFV-TP; a–c) and daclatasvir (d and e): (a) electrostatic, (b) H-bond and (c) steric interactions present between nsp12 and sofosbuvir-TP, and (d) H-bond and (e) steric interactions present between nsp12 and daclatasvir. (f) Representation of the predicted complex between the SARS-Cov-2 RNA and daclatasvir. (g) The H-bond interactions present between SARS-Cov-2 RNA and daclatasvir. The interactions are represented by black interrupted lines. The inhibitors and nsp12 residue structures are shown as stick models and are coloured by atom: the nitrogen atoms are shown in blue, the oxygen atoms are shown in red, the fluorine atoms are shown in purple and the carbon chain is shown in grey or cyan. Mg^{2+} ions are in green and nucleotides of the RNA template are represented as ball-and-stick models with CPK colouring. All the hydrogen atoms are omitted for clarity.

predictions from molecular modelling and the reduction of genomic/subgenomic cell-associated viral RNA synthesis, as well as the inhibition by daclatasvir of the reaction catalysed by the SARS-CoV-2 RdRp complex, led us to hypothesize that daclatasvir could structurally affect viral RNA. SARS-CoV-2 RNA displays secondary structures throughout its sequence, which are important during viral replication and transcription,[34] which can be monitored through melting curve analysis using a regular real-time thermocycler. Thus, a melting curve of extracted viral RNA was generated to assess whether daclatasvir could affect virus RNA folding.

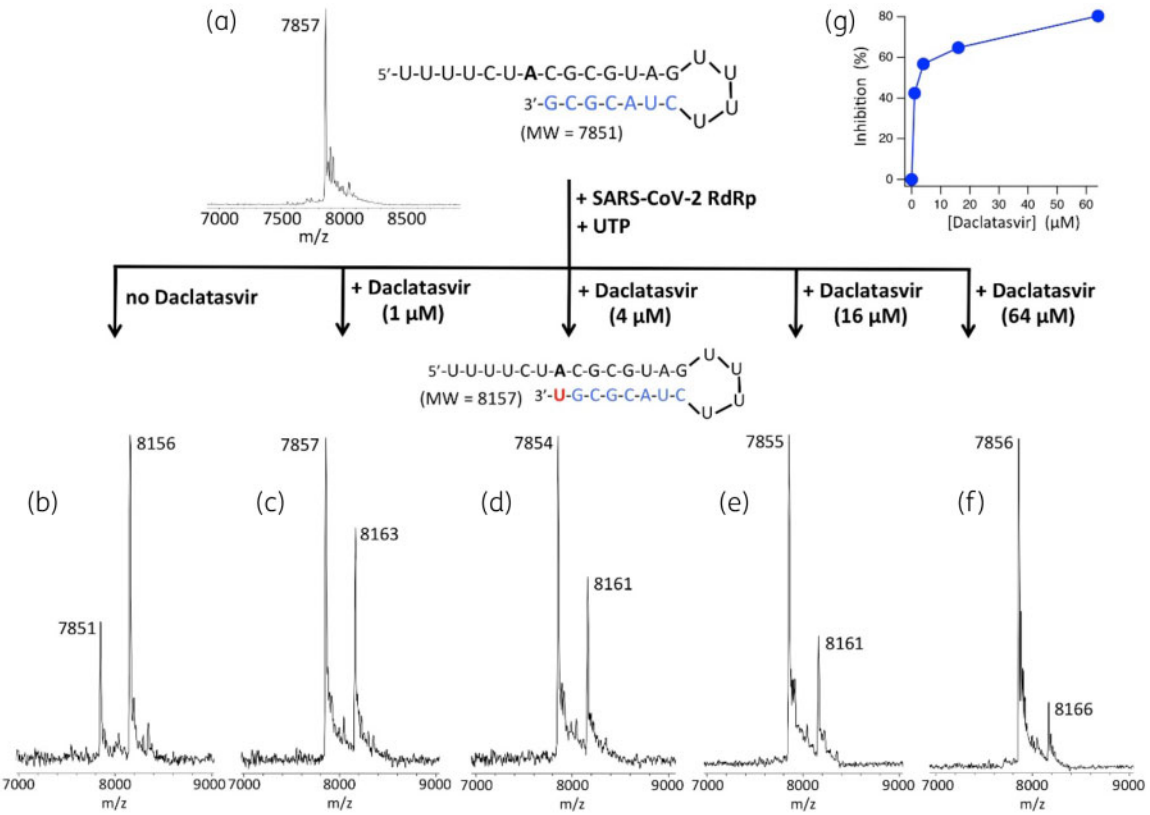

Figure 6. Inhibition of SARS-CoV-2 RdRp complex catalysed reaction by daclatasvir. A mixture of 500 nM RNA template-loop-primer (shown at the top of the figure), 1 μM SARS-CoV-2 pre-assembled RdRp complex (nsp12/nsp7/nsp8) and 3 μM UTP were incubated in buffer solution at 30°C for 1 h in the absence (b) or presence of daclatasvir at 1 μM (c), 4 μM (d), 16 μM (e) and 64 μM (f). The RNA template-loop-primer (a) and the products of the polymerase extension reaction (b–f) were analysed by MALDI-TOF MS. The signal intensity was normalized to the highest peak. The accuracy for m/z determination is ±10 Da. Reaction conditions were selected to yield an incorporation efficiency of approximately 70% as seen by MALDI-TOF-MS analysis in (b). The peak at 7851 Da corresponds to the RNA template-loop-primer (7851 Da expected) and the peak at 8156 Da corresponds to the U extended RNA product (8157 Da expected). Addition of daclatasvir reduced the amount of the U extended RNA product in a concentration-dependent manner. A plot for the inhibition of the polymerase reaction versus the daclatasvir concentration is shown in (g). This figure appears in colour in the online version of *JAC* and in black and white in the print version of *JAC*.

The thermal melting profiles of the RNA and RNA/daclatasvir complexes, obtained by varying the temperature, showed concentration-dependent effects favouring denaturation of the nucleic acid at low temperatures (Figure 7a and b), meaning that the structure of virus RNA is more easily disrupted in the presence of daclatasvir.

We further hypothesized that continuous culture of SARS-CoV-2 in the presence of daclatasvir may result in mutations in viral RNA that change the secondary structure pattern. Following 2 months of successive passages in Vero cells at an MOI of 0.1 in the presence of increasing concentrations, a 30% mutant subpopulation was detected in the presence of 7 μM daclatasvir (Figure 7c). A putative secondary structure at positions 28169–28259 of the SARS-CoV-2 genome was changed in the mutant virus in comparison with WT (virus grown in parallel without treatment) (Table 2 and Figure 7d and e; GenBank MT827075, MT827190, MT827872, MT827940, MT827074, MT827202, MT835026, MT835027, MT835383 and SRR12385359 and its coverage in Figure S5). Positions 28169–28259 are located at the junction between ORF8 and the N gene; thus, the change in the shape of the secondary RNA structure may prevent the binding of specific components required for the transcription of these genes (Figure 7d and e). Moreover, the low sequence identity of the mutant with SARS-CoV-2 genomes in GenBank suggests that it may be unlikely that mutant virus possesses adequate fitness (Table 2), which is in line with the observed reduction in virus infectious titres. SARS-CoV-2 grown in Vero cells with 7 μM daclatasvir was retested against this drug and, indeed, remained susceptible to this drug's antiviral effect (Table 2).

PBPK modelling for daclatasvir

A recent analysis of drugs proposed for repurposing as SARS-CoV-2 antivirals revealed that very few of the proposed candidates achieved their target concentrations after administration of approved doses to humans.[35] Moreover, there have been several recent calls to integrate understanding of pharmacokinetic principles into COVID-19 drug prioritization.[36–38] Initial assessment of the plasma pharmacokinetics of sofosbuvir indicated that the concentrations able to inhibit SARS-CoV-2 replication *in vitro* were unlikely to be achievable after approved doses. However, inhibitory daclatasvir concentrations were close to those achieved following

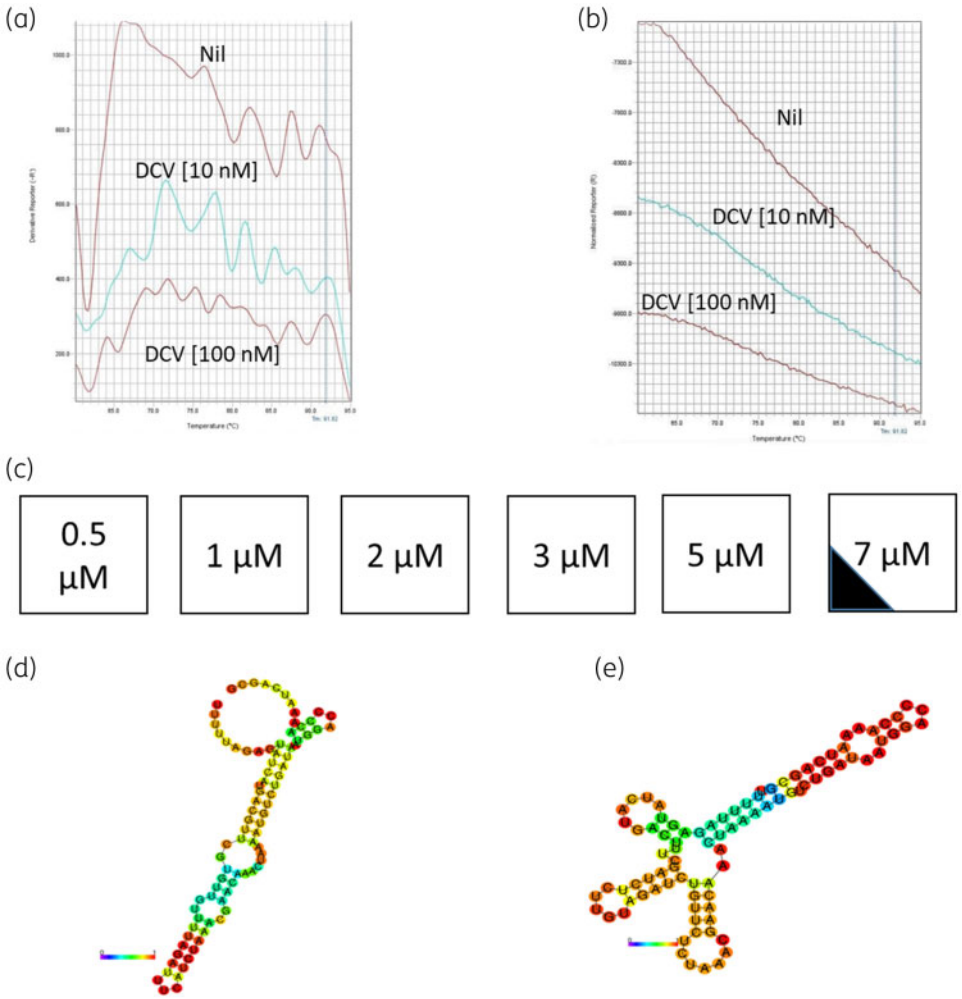

Figure 7. Daclatasvir favours SARS-CoV-2 RNA unfolding. A total of 10 ng of SARS-CoV-2 RNA was incubated with 10 or 100 nM daclatasvir (DCV) during a standard melting curve in the presence of picogreen; derivative (a) and normalized (b) reports are presented. (c) The scheme represents the percentage of WT (white) and mutant (black) virus after growing SARS-CoV-2 in Vero cells at a MOI 10 times higher than used in other experiments, 0.1, and sequentially treated with sub-optimal doses of daclatasvir. Each passage was done 2–4 days post-infection, when the cytopathic effect was evident. Virus RNA underwent unbiased sequencing using an MGI-2000 and a metatranscriptomics approach was employed during the analysis. WT (d) and mutant (e) SARS-CoV-2 secondary RNA structures encompassing the nucleotides 28169–28259 are presented. This figure appears in colour in the online version of *JAC* and in black and white in the print version of *JAC*.

Table 2. Genetic and biochemical characteristics of the daclatasvir-mutant SARS-CoV-2

Type	Sequence[a]	Secondary structure (dot bracket notation)	Thermodynamic ensemble (kcal/mol)	Identity to SARS-CoV-2 genomes	EC_{50} of daclatasvir (µM)
WT	TTTTTAGAGTATCATGACGTTCGTGTT GTTTTAGATTTCATCTAAACGA ACAAACTAAAATGTCTGATAATGGA CCCCAAAATCAGCG	.....(((((.((((((..((((..(((((((. . .)))))))..)))).....))))))))))).(((. . .))).	−17.67	99%	1.1 ± 0.3
Mutant	TTTTTAGAGTATCATGACTTTCGATCTCTTG TAGATCTGTTCTCTAAACGA ACAAACTAAAATGTCTGATAAT GGACCCCAAAATCAGCG	.((((((((((. . . . . .))). . .(((((. . . . .))))))(((((. . . . . .))))))..)))))))((.((((((..(((. . .))).))..))))))	−14.21	89%	1.0 ± 0.2

Mutations are underlined and an insertion is in bold.

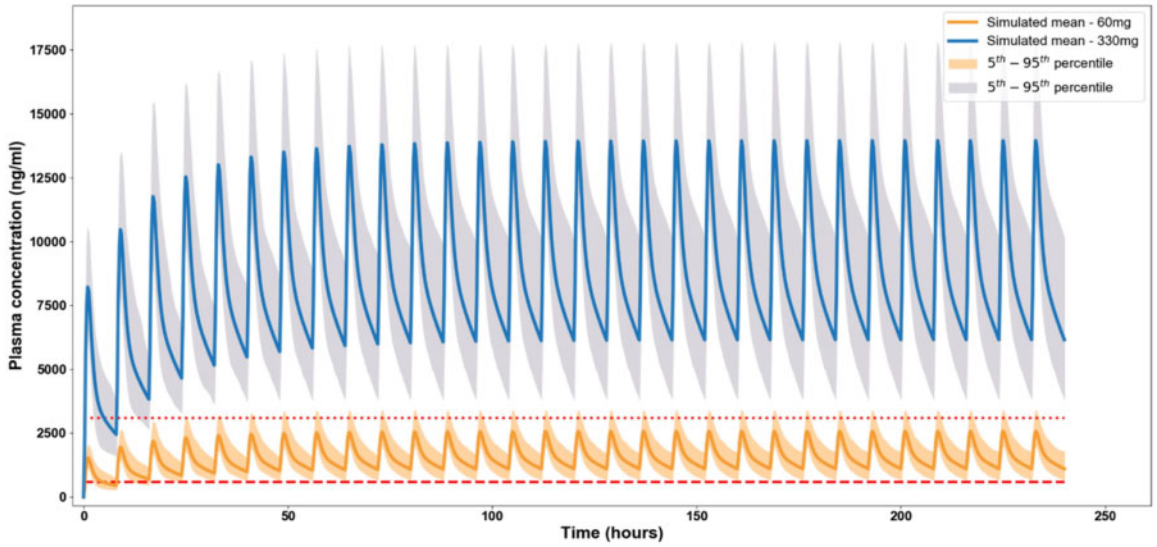

Figure 8. Predicted daclatasvir plasma concentration for multiple 60 mg and 330 mg thrice-daily doses. The dotted and the dashed lines represent the EC_{90} and EC_{50} values, respectively, of daclatasvir for SARS-CoV-2. This figure appears in colour in the online version of *JAC* and in black and white in the print version of *JAC*.

administration of its approved HCV dose. Therefore, PBPK modelling was used to estimate the dose and schedule of this drug to maximize the probability of success for COVID-19.

PBPK model validation against various single and multiple oral doses of daclatasvir had a ratio <2 between mean simulated and observed values and a summary of this shown in Tables S2 to S4. The average absolute fold error (AAFE) values for the observed versus simulated plasma concentration–time curve for a single 100 mg dose and multiple 60 mg once-daily doses were 0.92 and 0.76, respectively, and are shown in Figures S4 and S5. Thus, the known pharmacokinetic values and plots are in agreement with the expected range for the daclatasvir PBPK model, being considered as valid.

Figures S6 to S9 show the C_{24} values for various twice-daily and thrice-daily dose simulations, and 540 mg twice daily and 330 mg thrice daily were shown to satisfy systemic concentrations above the EC_{90} for at least 90% of the simulated population. Optimal dose was identified to be 330 mg thrice daily as this dosing regimen requires a lower dose per day than 540 mg twice daily. A comparison between 60 mg thrice-daily and 330 mg thrice-daily daclatasvir is shown in Figure 8 that satisfies C_{24} for EC_{50} (0.8 μM, 591 ng/mL) and EC_{90}, respectively, for treatment of SARS-CoV-2. This is a suggestion for dose escalation and tolerability studies; it does not represent an indication for clinical use.

Discussion

The COVID-19 pandemic continues to present a major concern to global health and is the most significant economic threat in decades.[2] SARS-CoV-2 actively replicates in type II pneumocytes, leading to cytokine storm and the exacerbation of thrombotic pathways.[31,39,40] Besides the virus-triggered pneumonia and sepsis-like disease associated with severe COVID-19, SARS-CoV-2 may reach the CNS[30] and liver.[41] Clinical trials with remdesivir suggest that early inhibition of SARS-CoV-2 replication may prevent severe COVID-19.[6,7] Thus, orally available and accessible medicines are necessary to overcome barriers that exist for remdesivir. Sofosbuvir and daclatasvir are considered safe and well tolerated anti-HCV therapies that are orally bioavailable. The presented work demonstrates: (i) SARS-CoV-2 is susceptible to daclatasvir; (ii) daclatasvir/sofosbuvir co-treatment shows a cooperative antiviral effect on SARS-CoV-2 replication in respiratory cells; (iii) sofosbuvir and daclatasvir prevented virus-induced neuronal apoptosis and release of cytokine storm-related mediators in monocytes, respectively; (iv) daclatasvir and sofosbuvir both inhibit the polymerase reaction catalysed by the SARS-CoV-2 RdRp complex via different mechanisms; (v) daclatasvir favours the unfolding of SARS-CoV-2 secondary RNA structures; and (vi) target concentrations of daclatasvir set by the *in vitro* activities are within the range that may be achievable in humans.

In the 9.6 kb genome of HCV, the gene *ns5a* encodes a multifunctional protein. The protein NS5A possesses motifs involved with lipid, zinc and RNA binding, phosphorylation and involvement in cell signalling events.[8] In viruses with less compact genomes, these functions and motifs are distributed to other proteins. For instance, in SARS-CoV-2, its 29 kb genome encodes: nsp3, with a zinc motif; nsp4 and 5, with lipidic binding activity; and nsp7, 8, 12, 13 and 14, able to bind RNA.[9] Although there is not a specific orthologue of NS5A in the SARS-CoV-2 genome, its activities may be exerted by multiple other proteins. Daclatasvir inhibited the production of infectious SARS-CoV-2 titres with EC_{50} values ranging from 0.6 to 1.1 μM across different cell types, including pneumocytes. Our experimental data clearly indicate that daclatasvir inhibits the polymerase reaction catalysed by the SARS-CoV-2 RdRp complex. Subsequent analysis illustrated that the daclatasvir mechanism of action could be, at least in part, associated with targeting viral RNA secondary structures, in line with the observation of lower infectivity in the absence of viral RNA decline in culture supernatant. SARS-CoV-2 possesses RNA pseudoknots that could contribute to the transcription processes[34] and daclatasvir-

associated denaturation of these structures could limit viral RNA polymerase activity. This already impaired catalysis may promote the cooperative polymerase reaction termination activity of sofosbuvir. This hypothesis warrants further investigation to confirm the mechanistic basis for the possible cooperation between sofosbuvir and daclatasvir in an *in vitro* model and clinically if observations from recent trials are confirmed.[42]

With relevance to sofosbuvir, we confirmed by enzymatic assays with SARS-CoV-2 RNA polymerase complex that sofosbuvir-TP acts as a chain terminator.[20,21] This activation process requires a multistage pathway in which hydrophobic protections in the sofosbuvir monophosphate are removed by the cellular enzymes CatA, CES1 and HINT, with subsequent engagement of nucleoside monophosphate and diphosphate kinase.[15] According to the Human Protein Atlas,[16–18] and functional assays with other pro-drug nucleotide ('ProTide') compounds,[43] these enzymes are also found in the respiratory tract. Indeed, we found that SARS-CoV-2 replication could be inhibited by sofosbuvir, at high concentration, in type II pneumocytes.

Sofosbuvir was able to prevent apoptosis in human neurons, whereas daclatasvir prevented the enhancement of IL-6 and TNF-α levels in human monocytes. These secondary mechanisms may also support cooperativity between sofosbuvir and daclatasvir, because neurological SARS-CoV-2 infection and cytokine storm are associated with poor clinical outcomes.[30,31] Another study also reported that sofosbuvir could be protective against neuro-COVID *in vitro*.[44] However, the authors analysed only a single concentration of 20 μM, which greatly exceeds the concentrations achieved by sofosbuvir after approved dosing to humans.[15] Here, neuroprotection is demonstrated to be promoted by sofosbuvir at 1 μM, which is closer to physiological concentrations.[15]

Based upon targets set by the *in vitro* pharmacological activity of daclatasvir, PBPK modelling indicated that systemic concentrations able to inhibit SARS-CoV-2 may be achievable in humans. Dose escalation may be needed to provide fully suppressive concentrations across the entire dosing interval, as has been shown to be needed for other viruses. However, the validity of such an approach would require careful assessment of safety and tolerability through Phase I evaluation of the higher doses. Furthermore, the prerequisite pharmacokinetic-pharmacodynamic relationships for successful anti-SARS-CoV-2 activity are yet to be unravelled and will likely require better understanding of the target-site penetration and free drug concentrations in matrices that recapitulate relevant compartments. Notwithstanding, the approved dose of daclatasvir (60 mg once daily) is low in relationship to other antiviral agents and the PBPK model provides posologies that may be reachable in dose-escalation trials.

In summary, effective early antiviral interventions are urgently required for the SARS-CoV-2 pandemic to improve patient clinical outcomes and disrupt transmission at the population level. The presented data for two widely available anti-HCV drugs, particularly for daclatasvir, provide a rational basis for further investigation of their safety at higher doses to meet the current needs of the COVID-19 indications.

Acknowledgements

Thanks are due to Professor Andrew Hill from the University of Liverpool and Dr James Freeman from GP2U Telehealth for simulative scientific debate. Dr Carmen Beatriz Wagner Giacoia Gripp from the Oswaldo Cruz Institute is acknowledged for assessments related to BSL3 facility. Dr Andre Sampaio from Farmanguinhos, platform RPT11M, is acknowledged for kindly donating Calu-3 cells. We thank the Haemotherapy Service of the Hospital Clementino Fraga Filho (Federal University of Rio de Janeiro, Brazil) for providing buffy-coats. We thank B. R. tenOever (Mt Sinai School of Medicine, New York, USA) for SARS-CoV-2 RNA, enabling expression plasmid preparation.

Funding

This work was supported by Conselho Nacional de Desenvolvimento Científico e Tecnológico (CNPq), Fundação de Amparo à Pesquisa do Estado do Rio de Janeiro (FAPERJ). This study was financed in part by the Coordenaçaõ de Aperfeiçoamento de Pessoal de Nível Superior—Brasil (CAPES) - Finance Code 001. Funding was also provided by CNPq, CAPES and FAPERJ through the National Institutes of Science and Technology Program (INCT) to Carlos Morel (INCT-IDPN). Thanks are due to Oswaldo Cruz Foundation/FIOCRUZ under the auspices of the Inova Program (B3-Bovespa funding). Funding was also provided by the Jack Ma Foundation, Columbia Engineering Member of the Board of Visitors Dr Bing Zhao and Fast Grants.

The funding sponsors had no role in: the design of the study; the collection, analyses or interpretation of data; the writing of the manuscript; or the decision to publish the results.

Transparency declarations

None to declare.

Author contributions

Experimental execution and analysis—CQS, NFR, JRT, SSGD, APDDS, CSS, ACF, MM, CRRP, CSF, VCS, FBS, MAF, CSGP, GV, LRQS, LGS, LVBH, TVAF, FSCB, MMB, RKRR, SJ, XW, CT, MC, WX, AG.

Data analysis, manuscript preparation and revision—CQS, NFR, JRT, NB, FAB, AO, MZG, SKR, DCBH, SJ, DP, TT, JJR, JJ, PTB, TMLS.

Conceptualized the experiments—CQS, NFR, JRT, JJ, TMLS.

Study coordination—TMLS.

Manuscript preparation and revision—DCBH, JJ, PTB, TMLS.

Supplementary data

Tables S1 to S4, Supplementary Materials and methods and Figures S1 to S9 are available as Supplementary data at *JAC* Online.

References

1 Cui J, Li F, Shi Z-L. Origin and evolution of pathogenic coronaviruses. *Nat Rev Microbiol* 2019; **17**: 181–92.

2 Dong E, Du H, Gardner L. An interactive web-based dashboard to track COVID-19 in real time. *Lancet Infect Dis* 2020; **20**: 533–4.

3 WHO. WHO R&D blueprint: informal consultation on prioritization of candidate therapeutic agents for use in novel coronavirus 2019 infection, Geneva, Switzerland, 24 January 2020. 2020. https://apps.who.int/iris/handle/10665/330680.

4 WHO Solidarity Trial Consortium. Repurposed antiviral drugs for COVID-19 – interim WHO SOLIDARITY trial results. *medRxiv* 2020; 2020.10.15.20209817.

5 Wang Y, Zhang D, Du G *et al.* Remdesivir in adults with severe COVID-19: a randomised, double-blind, placebo-controlled, multicentre trial. *Lancet* 2020; **395**: 1569–78.

6 Goldman JD, Lye DCB, Hui DS *et al*. Remdesivir for 5 or 10 days in patients with severe Covid-19. *N Engl J Med* 2020; **383**: 1827–37.

7 Beigel JH, Tomashek KM, Dodd LE *et al*. Remdesivir for the treatment of Covid-19 — final report. *N Engl J Med* 2020; **383**: 1813–26.

8 Smith MA, Regal RE, Mohammad RA. Daclatasvir: a NS5A replication complex inhibitor for hepatitis C infection. *Ann Pharmacother* 2016; **50**: 39–46.

9 Gordon DE, Jang GM, Bouhaddou M *et al*. A SARS-CoV-2-human protein-protein interaction map reveals drug targets and potential drug-repurposing. *bioRxiv* 2020; 2020.03.22.002386.

10 Keating GM. Sofosbuvir: a review of its use in patients with chronic hepatitis C. *Drugs* 2014; **74**: 1127–46.

11 de Freitas CS, Higa LM, Sacramento CQ *et al*. Yellow fever virus is susceptible to sofosbuvir both in vitro and in vivo. *PLoS Negl Trop Dis* 2019; **13**: e0007072.

12 Ferreira AC, Reis PA, de Freitas CS *et al*. Beyond members of the *Flaviviridae* family, sofosbuvir also inhibits chikungunya virus replication. *Antimicrob Agents Chemother* 2019; **63**: e01389–18.

13 Ferreira AC, Zaverucha-do-Valle C, Reis PA *et al*. Sofosbuvir protects Zika virus-infected mice from mortality, preventing short- and long-term sequelae. *Sci Rep* 2017; **7**: 9409.

14 Sacramento CQ, de Melo GR, de Freitas CS *et al*. The clinically approved antiviral drug sofosbuvir inhibits Zika virus replication. *Sci Rep* 2017; **7**: 40920.

15 EMA. Sovaldi. http://www.ema.europa.eu/docs/en_GB/document_library/EPAR__Public_assessment_report/human/002798/WC500160600.pdf.

16 The Human Protein Atlas. Tissue Expression of CTSA - Staining in Lung. https://www.proteinatlas.org/ENSG00000064601-CTSA/tissue/lung.

17 The Human Protein Atlas. Tissue Expression of CES1 - Summary. https://www.proteinatlas.org/ENSG00000198848-CES1/tissue.

18 The Human Protein Atlas. Tissue Expression of HINT1 - Summary. https://www.proteinatlas.org/ENSG00000169567-HINT1/tissue.

19 Gao Y, Yan L, Huang Y *et al*. Structure of the RNA-dependent RNA polymerase from COVID-19 virus. *Science* 2020; **368**: 779–82.

20 Gordon CJ, Tchesnokov EP, Woolner E *et al*. Remdesivir is a direct-acting antiviral that inhibits RNA-dependent RNA polymerase from severe acute respiratory syndrome coronavirus 2 with high potency. *J Biol Chem* 2020; **295**: 6785–97.

21 Ju J, Kumar S, Li X *et al*. Nucleotide analogues as inhibitors of viral polymerases. *bioRxiv* 2020; 2020.01.30.927574.

22 CDC. Coronavirus Disease 2019 (COVID-19). 2020. https://www.cdc.gov/coronavirus/2019-ncov/lab/rt-pcr-panel-primer-probes.html.

23 Wölfel R, Corman VM, Guggemos W *et al*. Virological assessment of hospitalized patients with COVID-2019. *Nature* 2020; **581**: 465–9.

24 Chien M, Anderson TK, Jockusch S *et al*. Nucleotide analogues as inhibitors of SARS-CoV-2 polymerase, a key drug target for COVID-19. *J Proteome Res* 2020; **19**: 4690–7.

25 Chen J, Malone B, Llewellyn E *et al*. Structural basis for helicase-polymerase coupling in the SARS-CoV-2 replication-transcription complex. *bioRxiv* 2020; 2020.07.08.194084.

26 Thomsen R, Christensen MH. MolDock: a new technique for high-accuracy molecular docking. *J Med Chem* 2006; **49**: 3315–21.

27 Zhang K, Zheludev IN, Hagey RJ *et al*. Cryo-electron microscopy and exploratory antisense targeting of the 28-kDa frameshift stimulation element from the SARS-CoV-2 RNA genome. *bioRxiv* 2020; 2020.07.18.209270.

28 Montgomery M, Ho N, Chung E *et al*. Daclatasvir (Daklinza): a treatment option for chronic hepatitis C infection. *P T* 2016; **41**: 751–5.

29 Kaletra (Lopinavir/Ritonavir) Dosing, Indications, Interactions, Adverse Effects, and More. https://reference.medscape.com/drug/kaletra-lopinavir-ritonavir-342629.

30 Asadi-Pooya AA, Simani L. Central nervous system manifestations of COVID-19: a systematic review. *J Neurol Sci* 2020; **413**: 116832.

31 Zhou F, Yu T, Du R *et al*. Clinical course and risk factors for mortality of adult inpatients with COVID-19 in Wuhan, China: a retrospective cohort study. *Lancet* 2020; **395**: 1054–62.

32 Ju J, Li X, Kumar S *et al*. Nucleotide analogues as inhibitors of SARS-CoV polymerase. *Pharmacol Res Perspect* 2020; **8**: e00674.

33 Jockusch S, Tao C, Li X *et al*. Sofosbuvir terminated RNA is more resistant to SARS-CoV-2 proofreader than RNA terminated by remdesivir. *Sci Rep* 2020; **10**: 16577.

34 Rangan R, Zheludev IN, Hagey RJ *et al*. RNA genome conservation and secondary structure in SARS-CoV-2 and SARS-related viruses: a first look. *RNA* 2020; **26**: 937–59.

35 Arshad U, Pertinez H, Box H *et al*. Prioritization of anti-SARS-Cov-2 drug repurposing opportunities based on plasma and target site concentrations derived from their established human pharmacokinetics. *Clin Pharmacol Ther* 2020; **108**: 775–90.

36 Zeitlinger M, Koch BCP, Bruggemann R *et al*. Pharmacokinetics/pharmacodynamics of antiviral agents used to treat SARS-CoV-2 and their potential interaction with drugs and other supportive measures: a comprehensive review by the PK/PD of Anti-Infectives Study Group of the European Society of Antimicrobial Agents. *Clin Pharmacokinet* 2020; **59**: 1195–216.

37 Venisse N, Peytavin G, Bouchet S *et al*. Concerns about pharmacokinetic (PK) and pharmacokinetic-pharmacodynamic (PK-PD) studies in the new therapeutic area of COVID-19 infection. *Antiviral Res* 2020; **181**: 104866.

38 Alexander SPH, Armstrong JF, Davenport AP *et al*. A rational roadmap for SARS-CoV-2/COVID-19 pharmacotherapeutic research and development: IUPHAR Review 29. *Br J Pharmacol* 2020; **177**: 4942–66.

39 Lin L, Lu L, Cao W *et al*. Hypothesis for potential pathogenesis of SARS-CoV-2 infection-a review of immune changes in patients with viral pneumonia. *Emerg Microbes Infect* 2020; **9**: 727–32.

40 Li H, Liu L, Zhang D *et al*. SARS-CoV-2 and viral sepsis: observations and hypotheses. *Lancet* 2020; **395**: 1517–20.

41 Wang Y, Liu S, Liu H *et al*. SARS-CoV-2 infection of the liver directly contributes to hepatic impairment in patients with COVID-19. *J Hepatol* 2020; **73**: 807–16.

42 HCV Drugs Sofosbuvir, Daclatasvir Show Promise as Potential COVID-19 Treatment. https://www.healio.com/news/infectious-disease/20200709/hcv-drugs-sofosbuvir-daclatasvir-show-promise-as-potential-covid19-treatment.

43 Pruijssers AJ, George AS, Schäfer A *et al*. Remdesivir inhibits SARS-CoV-2 in human lung cells and chimeric SARS-CoV expressing the SARS-CoV-2 RNA polymerase in mice. *Cell Rep* 2020; **32**: 107940.

44 Mesci P, Macia A, Saleh A *et al*. Sofosbuvir protects human brain organoids against SARS-CoV-2. *bioRxiv* 2020; 2020.05.30.125856.